AD-A172 087 HIGH POWER MODULATOR(U) PULSE SCIENCES INC SAN LEANDRO 1/1
CA R CURRY ET AL. AUG 86 PSI-FR-255 N00014-86-C-2020

UNCLASSIFIED F/G 9/5 NL

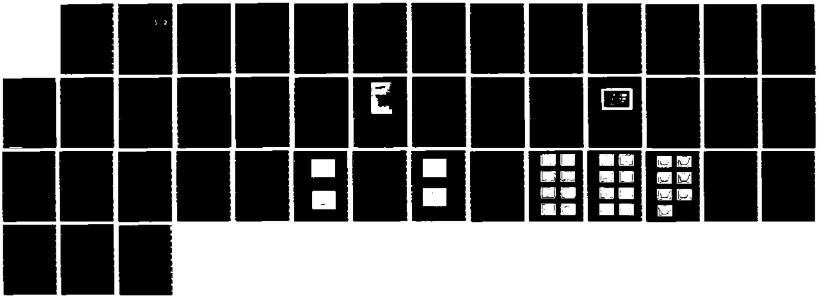

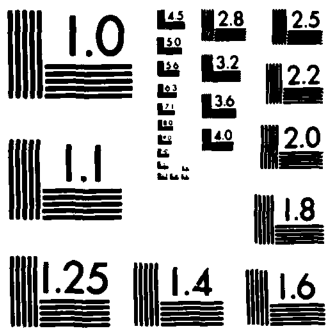

MICROCOPY RESOLUTION TEST CHART
NATIONAL BUREAU OF STANDARDS-1963-A

(12)

AD-A172 087

HIGH POWER MODULATOR
FINAL REPORT

PSI-FR-255

AUGUST 1986

R. CURRY, C. EICHENBERGER, D. MORTON,
AND L. SCHLITT

WORK SPONSORED BY

NAVAL RESEARCH LABORATORY
WASHINGTON, D.C. 20375

UNDER CONTRACT NO. N00014-86-C-2020

PREPARED BY

PULSE SCIENCES INC.
14796 Wicks Blvd. • San Leandro, CA 94577
Tel: (415) 895-2984

HIGH POWER MODULATOR
FINAL REPORT

PSI-FR-255

AUGUST 1986

R. CURRY, C. EICHENBERGER, D. MORTON,
AND L. SCHLITT

WORK SPONSORED BY

NAVAL RESEARCH LABORATORY
WASHINGTON, D.C. 20375

UNDER CONTRACT NO. N00014-86-C-2020

PREPARED BY

PULSE SCIENCES, INC.
14796 WICKS BLVD.
SAN LEANDRO, CA 94577

TABLE OF CONTENTS

1.0 INTRODUCTION

This report describes the High Power Modulator (HPM) which was constructed for the Naval Research Laboratory (NRL) by Pulse Sciences Incorporated of San Leandro, California (PSI) in accordance with the specifications set forth in contract N00014-86-C-2020.

The nominal electrical specifications for the HPM were to produce a 1 µs flattop (± 3%) pulse with a minimum amplitude of 200 kV into a 400 ohm resistive load but with a design goal of 250 kV. The HPM meets or exceeds the design goals.

The HPM has three modes of operation; 1) single shot, 2) continuous repetitive at rates up to 1 Hz, and 3) burst for up to 50 pulses at rates up to 100 Hz. The operating modes as well as their associated parameters are switch selectable through a sophisticated control system.

The HPM control system incorporates fault detection circuitry which identifies open and short circuit load conditions and automatically terminates a sequence of requested pulses when these conditions occur. The circuitry is capable of preventing a subsequent pulse from being fired even at a 100 Hz repetition rate.

Section 2 contains a description of the HPM. A brief chronology of the project is given in Section 3. The testing of the HPM during its development, its acceptance at PSI, and its acceptance at NRL is described in Section 4.

2.0 SYSTEM DESCRIPTION

2.1 Introduction

A compact 250 kV modulator has been designed to provide flat 1 μsec pulses into a 400 Ω electron beam load during 100 pps, burst mode operation. The modulator was designed around a 15:1 step-up transformer thus providing a compact design. To satisfy the desired stringent flatness specification of ± 3% with a slightly varying load impedance, the 1 μsec, 625 A output pulse is generated by a tunable low inductance, low impedance type E PFN. The modulator is able to provide up to 50 pulses at 100 pps or continuous operation at 1 pps. The oil insulated output pulse transformer has multiple secondary windings which can be used to provide heater power for a thermionic cathode electron beam source. The resonantly charged 1.8 Ω PFN is constructed in a folded stripline arrangement to reduce stray inductance. The 10 kA, 33 kV primary discharge pulse is switched by a high current, hollow anode thyratron, EEV CX1574C.

The control system allows the operator to select a given set of run parameters including pulse repetition frequency and the number of pulses in a burst. During operation the control system detects fault mode conditions, and provides automatic shutdown in case of open circuit or short circuit conditions.

Traditionally, modulators may range from several kilovolts up to the megavolt range. In the 20 kV - 100 kV range the modulators are usually either thyratron switched or switched by a high current gas spark gap. Until recently high average current thyratrons which could handle large voltage reversals were not commercially available. Rather, standard thyratrons were used and protection circuits were designed into the modulator. Spark gaps were usually more attractive in these high reversal operating

regimes or as the peak currents increased over 10 kA (repetitive rates < 1 kHz).

New thyratrons developed for use in excimer laser drivers avoid many of the limitations of the standard thyratron. These new hollow anode, ceramic thyratrons are able to handle 50-60% current reversal, without suffering lifetime decreases.[1] This advantage is quite important for modulators intended for applications other than laser drivers. For example, in many modulators driving diode or e- beam sources, open circuit or short circuit fault modes are usually present. Open circuit conditions can occur as the diode emitting material ages or as the diode conditions initially. Inherently short circuit conditions can easily be encountered. The vacuum diode region may occasionally short out if the diode arcs, the vacuum bushing flashes, or if premature plasma closure occurs. All of these fault modes effect the lifetime of the modulator. Short circuit conditions can result in high peak current reversals in the circuit as well as depleting the cathode of the thyratron.

A compact 250 kV modulator has been designed by Pulse Sciences Inc. (PSI) which can easily operate under these stringent conditions. The modulator was designed as a general purpose driver for a high impedance thermionic diode. The modulator was delivered as a turn-key system complete with integral oil pumping and storage capability. A partial block diagram (Figure 1) illustrates some of the key features of the system. An automatic control system capable of monitoring all essential conditions of the ancilliary support equipment and fault modes was designed into the system. Although the control system is discussed in a following section, a brief summary is required before proceeding. Because the modulator was designed as a stand-alone test facility for diode development, complete automatic control was required. The control system was designed to monitor and control charging voltage,

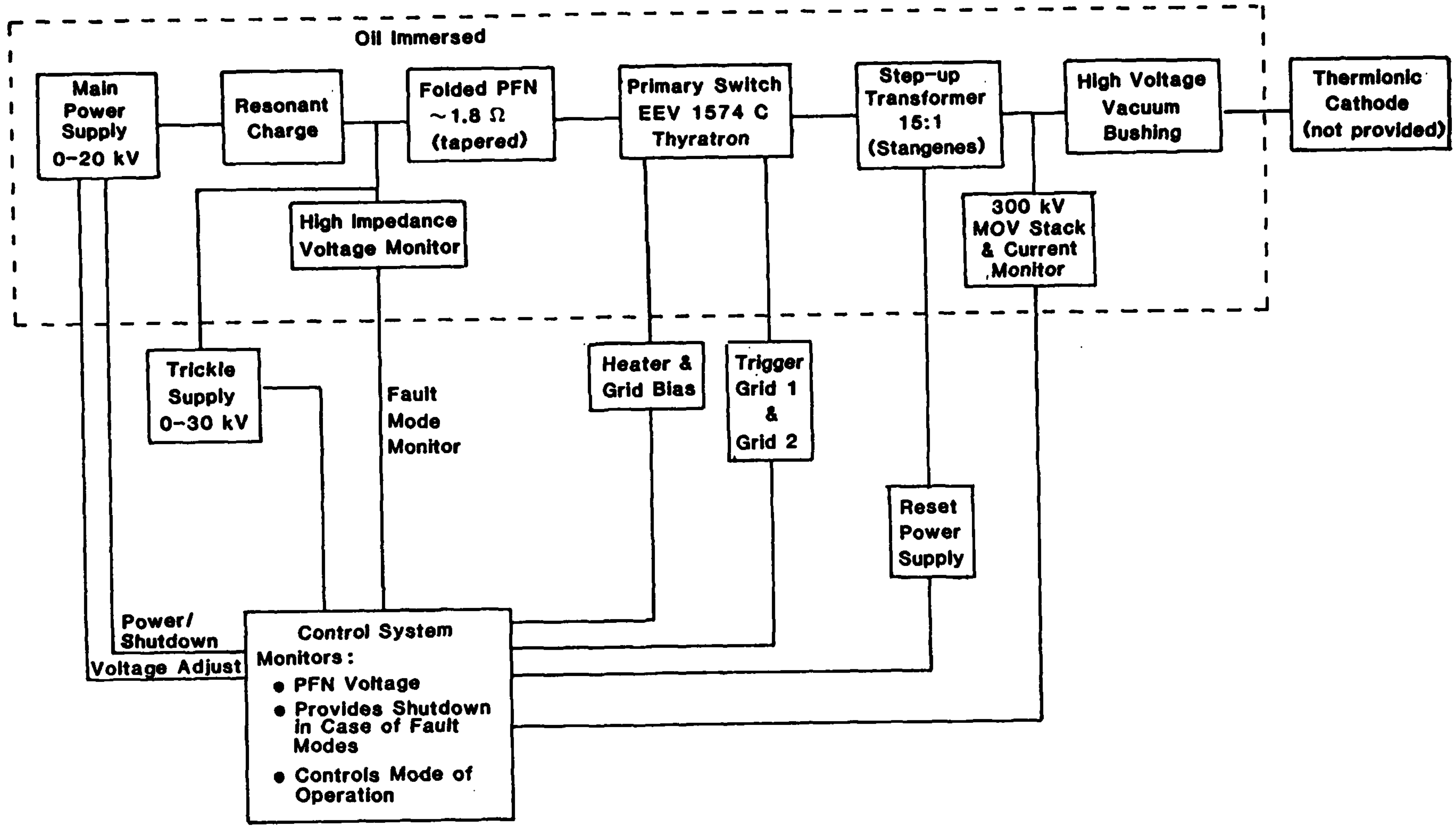

FIGURE 1. Block diagram of the modulator and support systems.

detect short circuit and open circuit conditions, and provide shutdown in case of reoccuring fault modes. In addition, the control system was designed to monitor the status of the ancilliary equipment (reset supply, PFN charge voltage, etc.) and provide shutdown to avoid damage to the key components of the system including the thyratron, the step-up transformer, the main power supply and the high voltage bushing. To illustrate the complexity and the key design issues, the following sections provide a detailed discussion of the modulator and controls.

2.2 Modulator Description

The modulator was designed to provide 50 - 250 kV, 1 μs pulses to a 400 Ω load. The design utilized a 35 kV, 15 kA hollow anode thyratron (EEV 1574C) to discharge a 1.8 Ω tapered pulse forming network through an iron core pulse transformer (Figure 2). The pulse forming network was resonantly charged from a 5 μF capacitor, DC charged to approximately 17 kV. To provide for single pulse operation, a trickle charge supply, adjustable from 0 - 35 kV was also provided.

The main power supply was sized to provide for interpulse recharge of the previously mentioned 5 μF capacitor. The 30 kW power rating of the supply recharged the 5 μF capacitor in approximately 10 ms, which was adequate for the 10 ms interpulse period. The PFN was resonantly charged through a 0.8 H inductor provided in the system. At high rep-rates the power supply regulated the PFN voltage to ± 3%. At slightly reduced rep-rates, the regulation of the supply performed to better than ± 1.5%.

The thyratron (EEV 1574C) was selected for peak voltage hold- off, peak current and the ability to conduct high reverse currents. The thyratron was rated at peak currents of 15 kA and 7.5 kA reverse currents. Lifetime tests published on 11 kA opera-

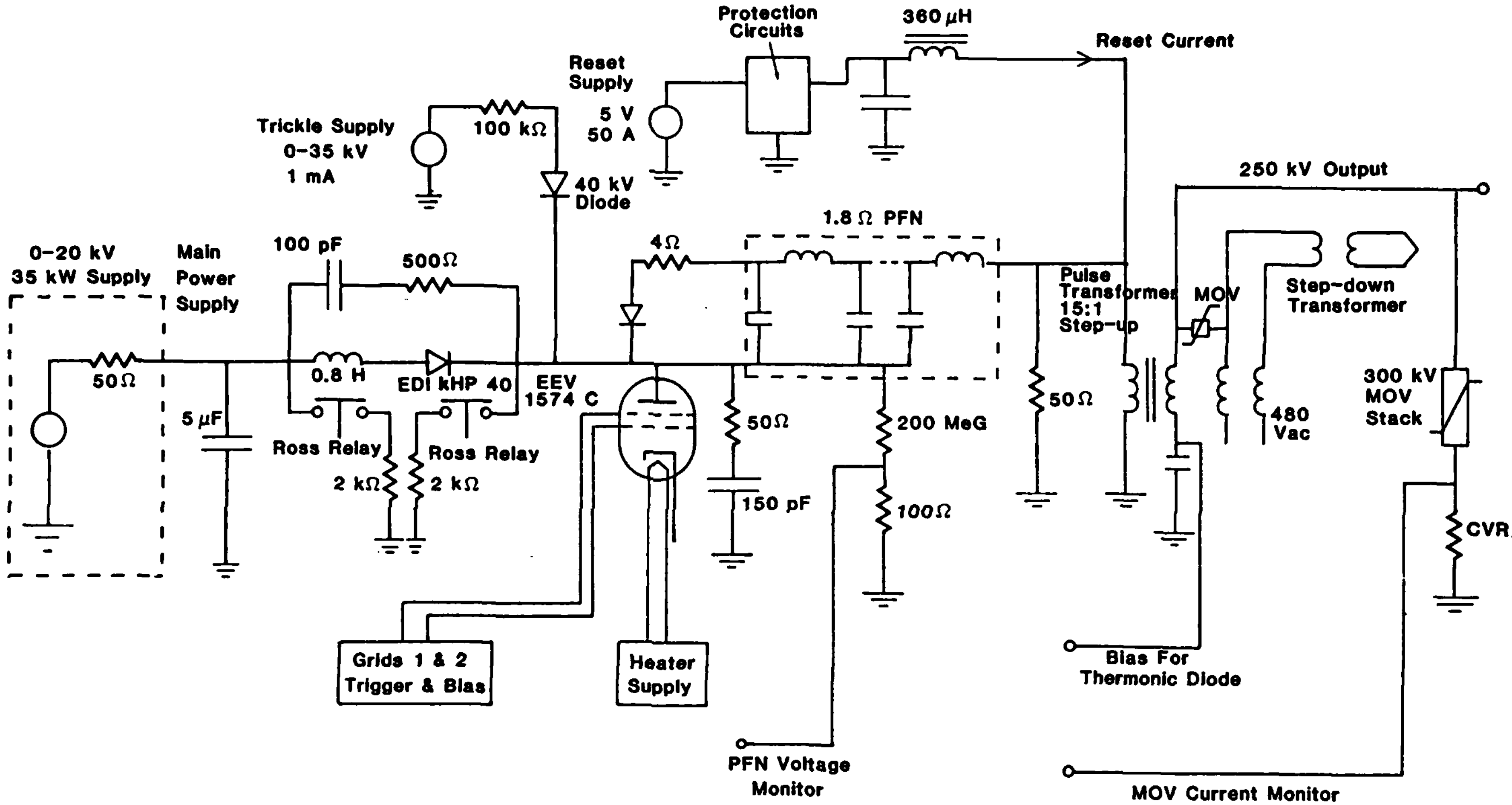

FIGURE 2. Schematic of 250 kV modulator, showing the resonant charge system, PFN and some of the protection circuitry designed into the modulator.

ting conditions, reported minimum lifetimes in excess of 1×10^8 shots[1] at 11 kA and di/dt's of 2×10^{11} A/sec. In addition, the thyratron had also been tested at 500 pps. Design goals of 1×10^6 shots with 10 kA peak currents and an anticipated di/dt = 5×10^{10} A/sec at 100 pps were well within the thyratron specification test parameters. During short circuit fault modes, large reverse currents (10-12 kA) could possible occur in the primary discharge loop. Although this was slightly higher than specification, tradeoff studies done, showed that the thyratron would conduct these reverse currents. The thyratron in the short circuit condition was also required to withstand several reversals until the voltage was damped out by the smaller diode circuit placed across the PFN (Figure 2).

A folded stripline, PFN was constructed to provide a low impedance, low inductance PFN required to drive the 400 Ω diode load through a step-up transformer. The pulse forming network, was a hybrid of the type-E PFN, and the Rayleigh PFNs.[(2)] The pulse forming network shown in Figure 3 illustrates this. The required flatness of ± 3% for a 1 microsecond pulse was not easily achieved, along with the desired risetime of 200 nanoseconds. The inductance of the selected capacitors (ESL) and the output capacitance of the step-up transformer interacted and further complicated the design tradeoffs. Originally, 7.5 nF reconstituted mica capacitors were selected for the PFN capacitors. The equivalent series inductance of the capacitors was specified to be less than 60 nH. Unfortunately, in house tests revealed approximate ESL's of 290 nH per capacitor. In low impedance PFNs, high ESL can dramatically effect the output pulse, resulting in early drop off and large variations in the pulse. Original circuit simulations had taken into account the 2% droop of the transformer and the large secondary stray capacitance (150 - 200 pF), and had shown that the high ESL would shorten the pulse. Early tests with the modulator revealed that the output

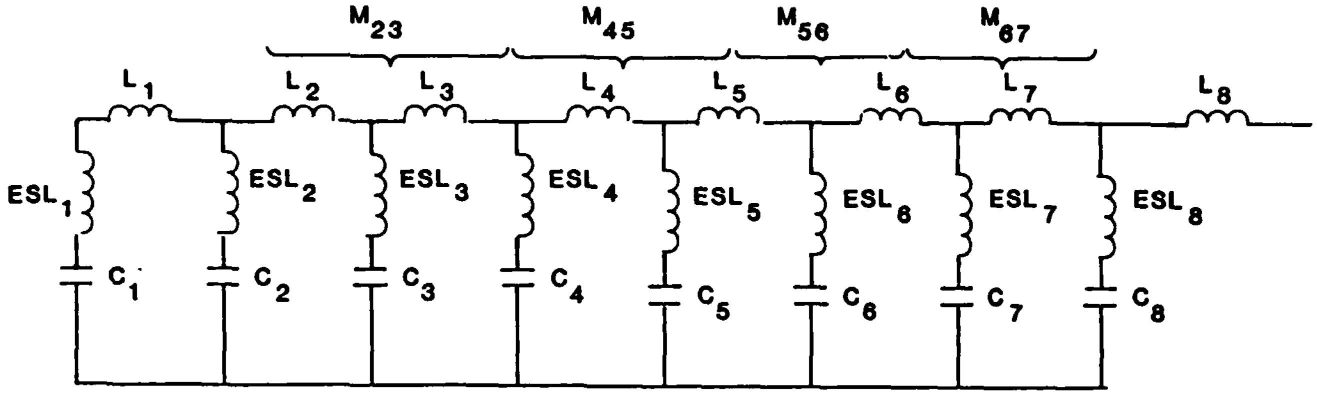

$C_1 - C_8$ 53 nF ± 5% (7 x 7.5 nF 35 kV capacitors)

$L_1 \simeq$ 25 nH (2-2 parallel 2" long 1/4" diameter pieces of wire)

$L_2 \simeq$ 137 nH (2 parallel coils, 3 turns each)

$L_3 \simeq$ 151 nH (2 parallel coils, 3 turns each)

$L_4 \simeq$ 167 nH (2 parallel coils, 3 turns each)

$L_5 \simeq$ 167 nH (3 parallel coils, 2-3 turn coils in parallel with a 4 turn coil)

$L_6 \simeq$ 167 nH (3 parallel coils, 2-3 turn coils in parallel with a 5 turn coil)

$L_7 \simeq$ 167 nH (3 parallel coils, 2-3 turn coils in parallel with a 5 turn coil)

$L_8 \simeq$ 280 nH, (includes the leakage inductance of the transformer and lead inductance)

$ESL_1 - ESL_8 \simeq 40$ nH

$M_{23} = M_{45} = M_{67} \simeq 10$ nH

FIGURE 3. Modified type-E PFN showing the approximate values of the section inductances.

pulse width was indeed shorter by 80 ns, 920 ns in duration. To compensate for the high series inductance (ESL) (Figure 3), an eighth section was added. Although the inductor of the extra section (Section 1) is not mutually coupled to the other inductors of the PFN, the extra section did extend the pulse width to the required 1 microsecond pulse width and the required flatness. Typically when an extra section is added to a PFN, droop in the pulse is normal. However, the stripline design of the PFN reduced the stray inductance in the network to a minimum (Figure 4) allowing the extra section to compensate for tail end droop. If the construction of the PFN is reviewed in Figure 4, the advantages of utilizing stripline construction is easily understood. The stripline produces a low inductance connection between capacitors and reduces the stray induction normally present in the intersection connections.

Each section of the network consisted of a module housing seven of the 7.5 nF capacitors. Three mounting holes were provided in the modules. Coils constructed from 1/4" copper tubing were used as the inductors, and mounted from these holes. Early inductance calculations using Nagoaka's inductance formulas and Terman's formulas showed that the inductances were not easily adjusted by varying the length of the coils.[3,4] A fairly unique solution was devised. Because the PFN was required to be tunable to compensate for load changes (different diode impedances) tunability was an important consideration. In addition to the low inductance provided by a stripline design, the low inductance mounting of the capacitors close to the section inductors allowed an additional inductor to tune the first few sections of the PFN. The third inductor introduced into the network was mounted between the two coils which set the primary section inductance. To help in the review of the PFN outline the currents are shown in Figure 4.

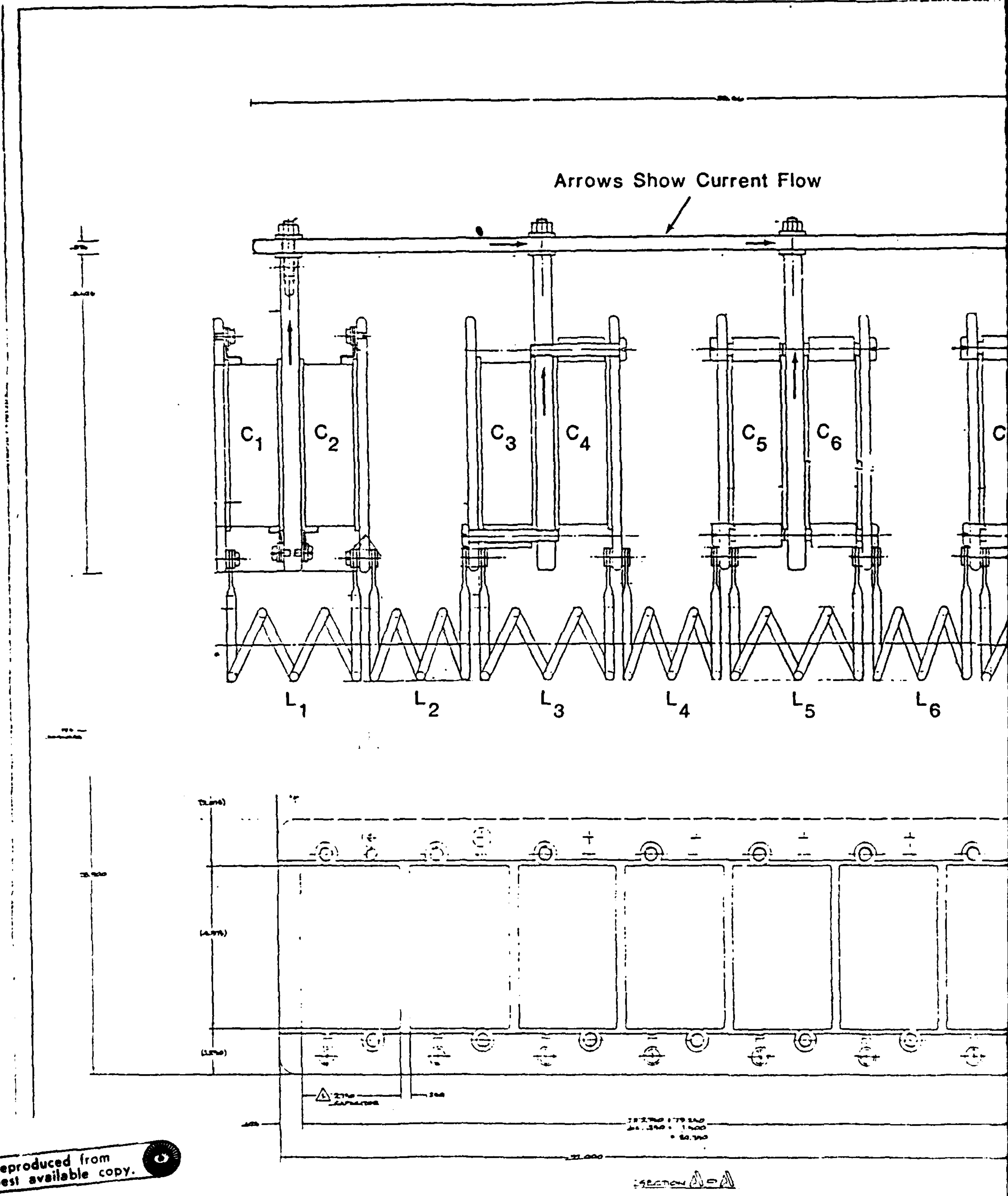

FIGURE 4. An outline drawing of the PFN showing the low inductance design of the PFN.

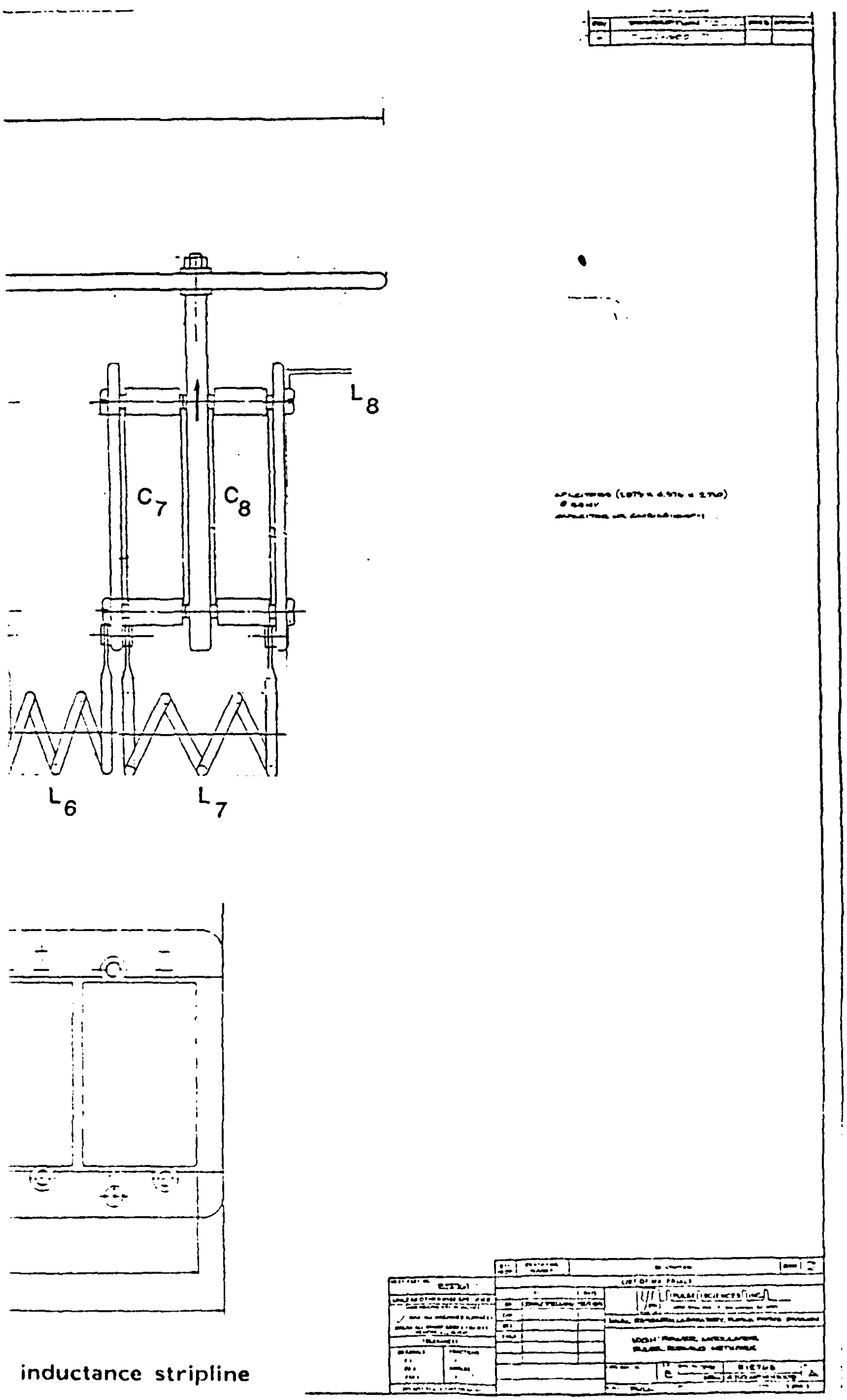

L8
C7
C8
L6
L7
inductance stripline

The output of the PFN was stepped up by 15:1 step-up transformer. In addition the iron core transformer provided matching between the 1.8-ohm PFN and the 400-ohm load. The transformer (manufactured by Stangenes Industries) was designed to provide a 1 μs, 250 kV pulse with less than 2.5% droop. To accommodate these specifications, the primary leakage inductance was approximately 106 nH. With the calculated output stray capacitance of 140 pF, the estimated risetime was 100 ns. The full ΔB swing of the core was utilized by biasing the primary with a reset current. A 55 A current from a 5 V power supply resets the transformer before each pulse. Protection circuitry provided isolation between the high voltage on the primary and the low voltage side of the supply. In addition, a quadfiliar secondary winding was provided to supply power to a 2 kW heater winding biased at -2 kV with respect to the 250 kV output pulse.

Fault mode protection circuits designed into the modulator, provided protection to the thyratron, the pulse transformer and the high voltage bushing. No clamping circuits were used across the thyratron. However, a snubber network was placed across the thyratron in the event of a fault mode (Figure 2). High voltage diodes along with series limiting resistors were placed across the PFN to prevent reversals from occuring on the PFN capacitors. Tests showed that the high voltage diodes were capable of conducting 10 kA currents and the 5×10^{10} A/sec di/dt's present. A metal oxide varistor stack consisting of 150 GE 1000 LA 80 MOV's was used to provide a matched load to the output of the transformer at 300 kV. No loading of the output pulse was noted at lower voltages, by the stack. Although the stack under normal operating conditions does not load the pulse, the MOV still has a finite lifetime under normal operating conditions. The calculated lifetime of the stack was approximately 1×10^6 shots. For long lifetime modulators this could conceivably be a problem. The

design goal of the modulator was 1×10^6 shots without maintenance. The estimated lifetime of the modulator was $1 \times 10^8 - 1 \times 10^9$ shots under rep-rate burst mode operation (excluding the MOV stack).

The circuit of Figure 2 was designed into four stages all modular in design. The modulator was housed in an oil tank mounted atop an oil reservoir (Figure 5). Associated controls were designed into self-contained rack mounted chassis. The power supply was provided in a heat sinked oil tank totally self-contained. The low inductance mounting and the layout of the modulator's internal components are shown in Figure 5. The oil tank, oil reservoir, rack mounted controls and the modulator frame are shown in the photograph in Figure 6.

The HPM incorporates a ceramic high voltage vacuum bushing with metal seals for compatibility with a wide range of thermionic cathodes. The bushing consists of three segments of alumina tubing with interspersed metal rings. All metallic surfaces exposed to vacuum are stainless steel with the exception of the seals themselves. Nylon bolts in the oil surrounding the bushing provide sufficient clamping force to permit use with indium wire seals and metal C-seals as well as with elastomer seals. During the tests at PSI, the bushing was assembled with buna-n elastomer seals and routinely achieved pressures below 2×10^{-6} Torr with an untrapped 4 inch diffusion pump. The bushing was delivered to NRL with indium wire seals and achieved pressures below 3×10^{-7} Torr. Indium coated C-seals are recommended for future use.

The bushing did flash occassionally during the development testing of the HPM. Flashovers did not cause detectable damage to the bushing which always recovered on subsequent shots. Ultimately the bushing was able to repeatedly withstand short transients in excess of 450 kV followed by 350 kV microsecond pulses during open circuit fault mode tests.

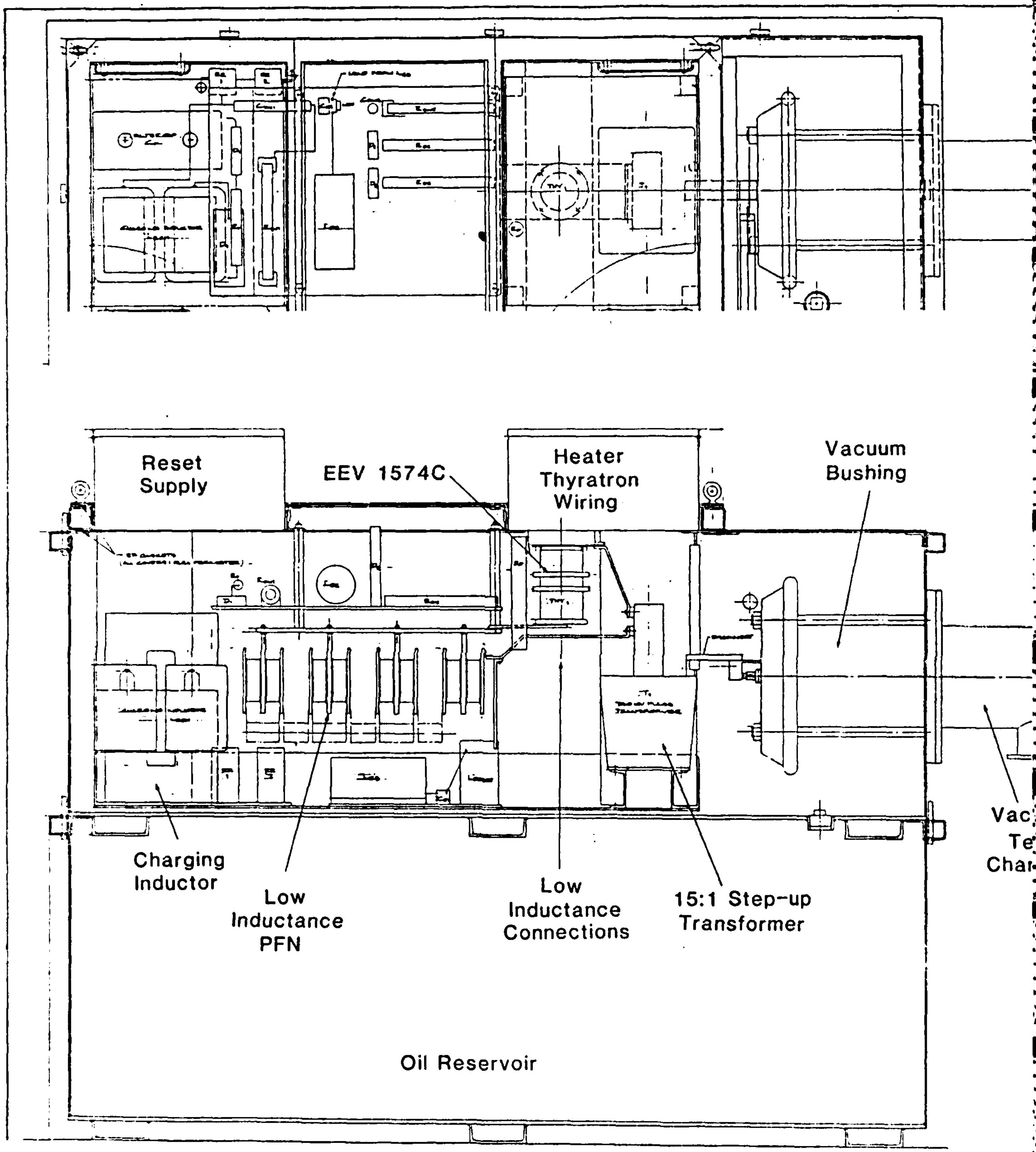

FIGURE 5. A cross section drawing of the modulator showing the low inductance co

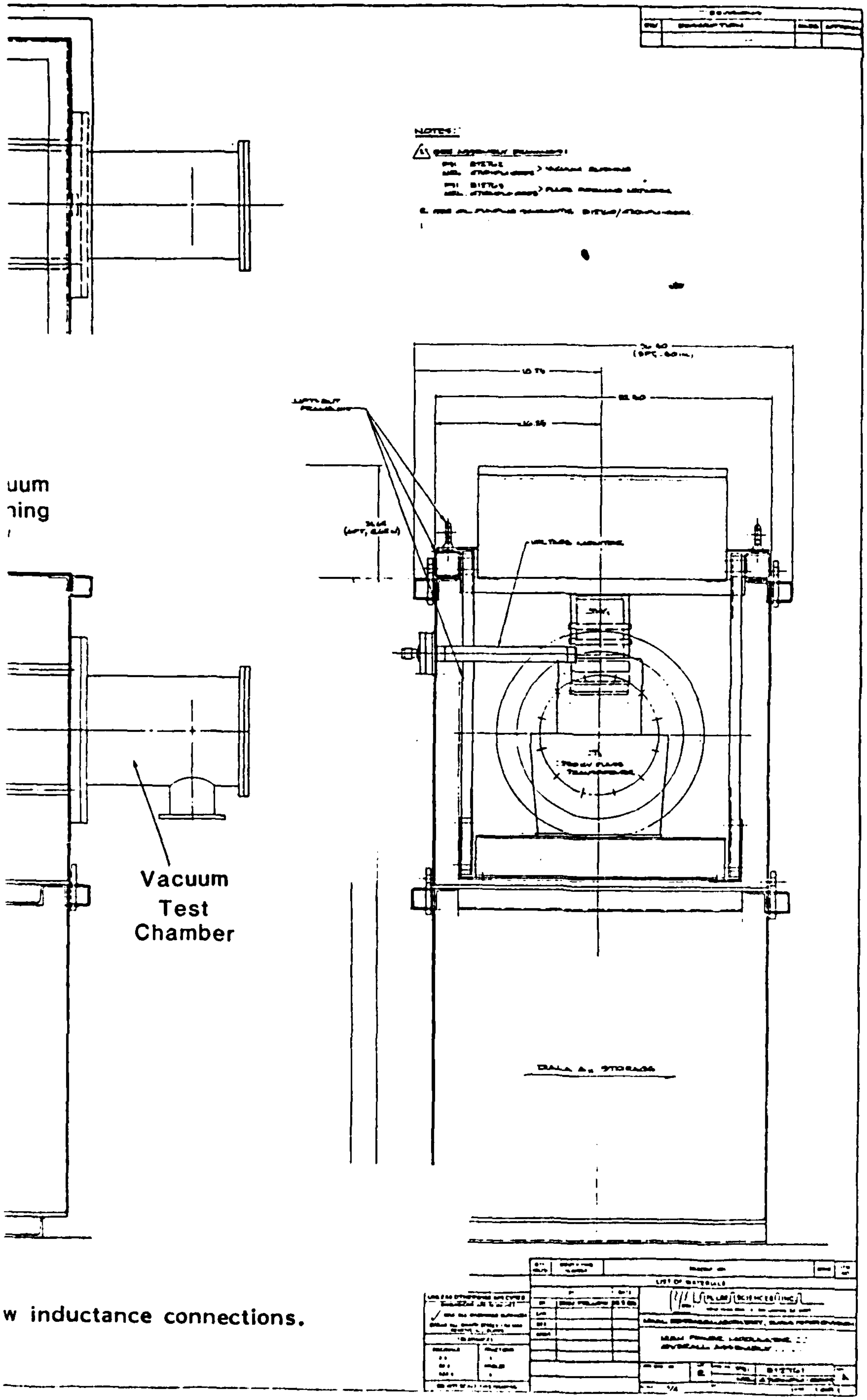

w inductance connections.

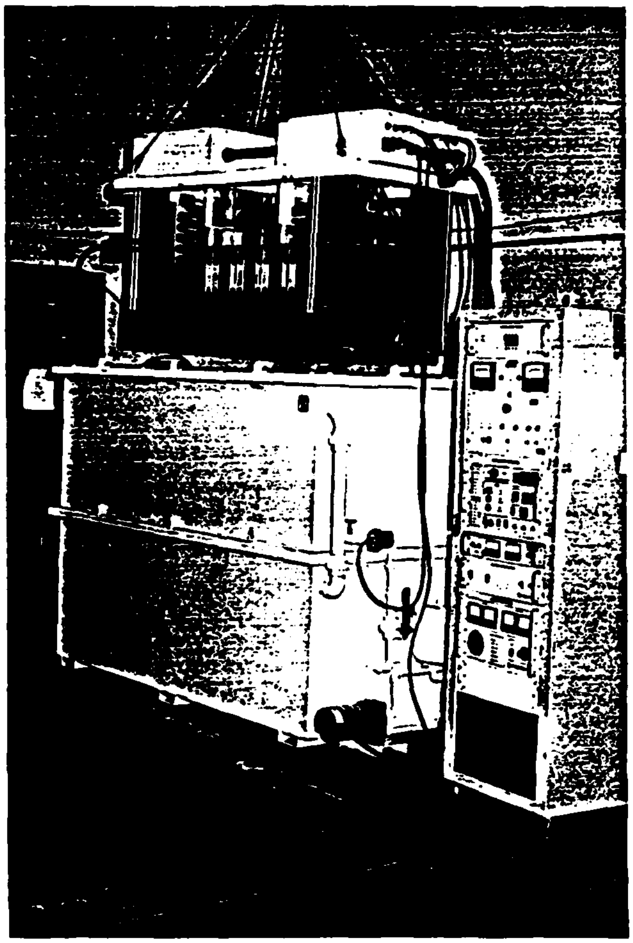

FIGURE 6. Photograph of the modulator and associated support hardware, showing the modulator (top) supported above the oil tank and reservoir. The control system is shown to the right.

2.3 Command, Control and Triggering System

The control and trigger system are housed primarily in a 19" rack. The system is divided into the system power control chassis, the 30 kW, 20 kV supply control chassis, the 30 W, 40 kV supply chassis, the thyratron heater/reservoir chassis, the system interconnect/junction chassis and the master control chassis (Figure 7). Additional elements are located in RFI boxes located on the modulator tank (Figure 5). The system incorporated proven techniques for noise suppression and immunity in pulsed power environments. The system was designed to allow integration into a larger system with a safety/interlock system.

The control system performs the following major functions:

- o Monitor and display of all safety interlocks.
- o Monitor and display of all support and sub-system interlocks.
- o Control and remote programming of all high voltage supplies.
- o Control and monitoring of all crowbars and clamps.
- o Generation and sequencing of all low-level trigger signals.
- o Control of all system parameters such as rep-rate, number of pulses, charge voltage, etc.
- o Display of system status.
- o Real time display of measured PFN voltage.

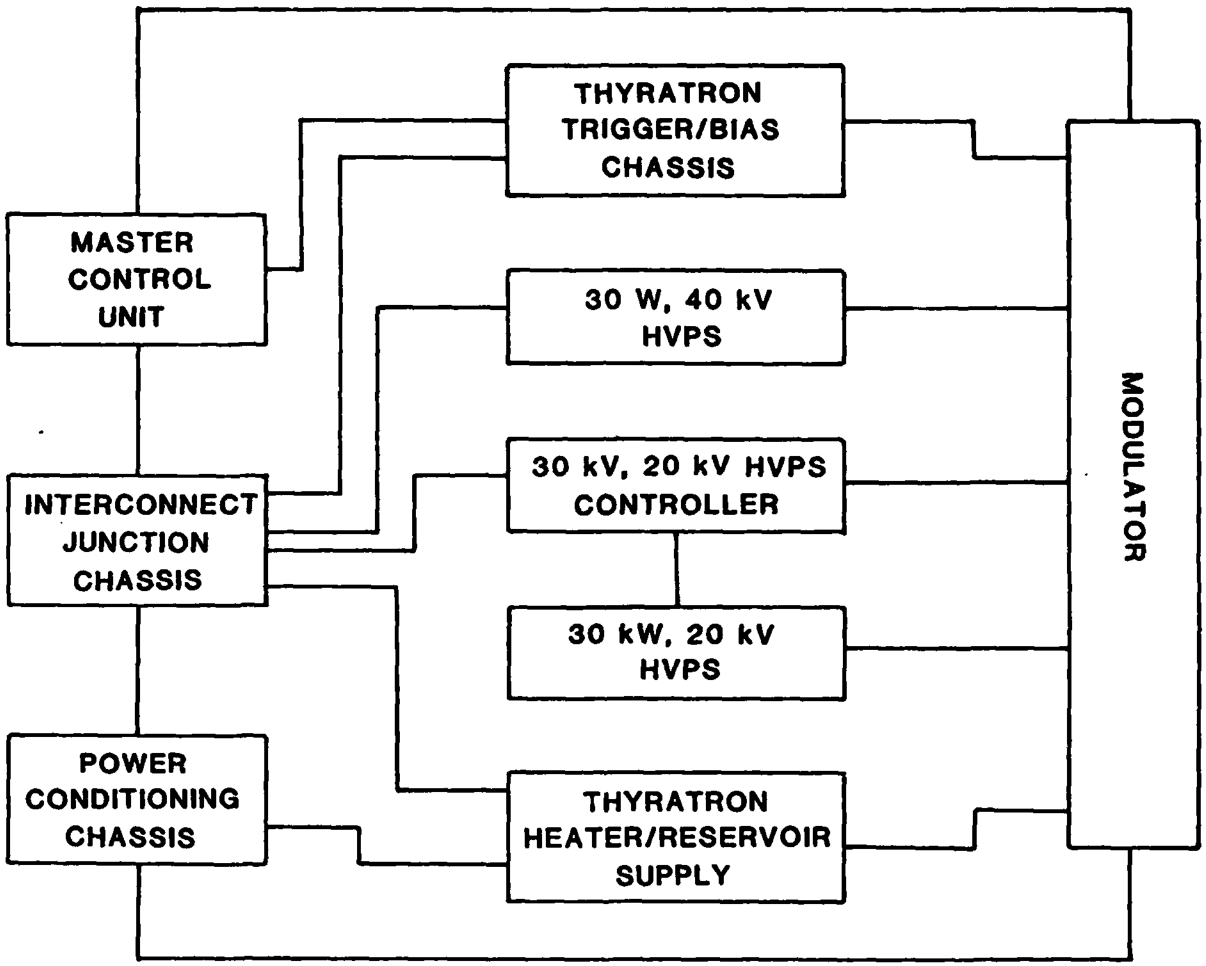

FIGURE 7. Block diagram showing the interconnections of the control system.

o Fault detection and auto-ABORT control functions.

o Orderly shutdown of all systems upon auto-ABORT command.

Figure 8 shows the main control panel and the functions monitored by the controller.

Conditions of all interlocks, fault detection circuitry and sub-systems are displayed realtime using tri-color LED's. Green denotes that the interlock is connected. Red denotes the interlock is not satisfied or broken, and yellow denotes that the interlock has been bypassed.

Selection of charge voltage, number of pulses and rep-rate is accomplished by the use of thumbwheel switches. Voltage and pulse resolution is 0.1 kV, 1 pulse and 0.1 Hz respectively. Both internal and external triggering is available but rep-rate is limited to 110 Hz maximum. A low jitter pulse arriving approximately 500 ns before system output is provided for timing. The front panel also displays the quantity of actual shots fired during a burst mode or single shot operation.

Three system modes are available; single shot, burst and slow-rep. The burst mode allows up to 99 pulses at up to 102 Hz using an internally generated or external pulse train. The slow-rep mode allows continuous operation at 1.2 Hz or less.

Realtime scaled digital display of measured PFN voltage is accomplished using a fast gated analog to digital converter/display unit triggered from a fire delay signal.

The system design approach incorporates features that limit single shot fault modes to energy/voltage levels within component specifications. Therefore, fault mode protection philosophy is

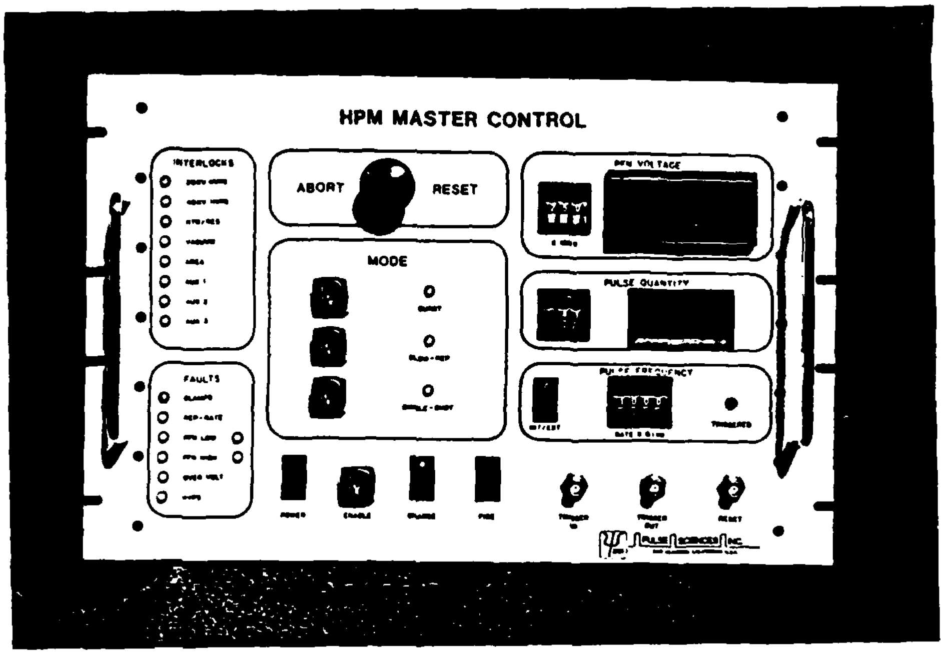

FIGURE 8. Photograph of the master control panel showing the functions performed by the control system.

based on prevention of subsequent pulses occuring where a repeat of the particular fault mode is likely. All fault modes detected are identified via front panel indicator displays. Fault levels are auto-scaled with requested PFN voltage, thus no external programming is required when operating at different voltages.

Auto-ABORT detection circuits for output high (load open), output low (load shorted), PFN high, PFN low (thyratron latchup), varistor stack overcurrent and power supply fault are provided which are fast enough to prevent a subsequent shot from being fired at the maximum rep-rate of 100 pps. The front panel indicators identify which circuit caused the auto-ABORT. Automatic control of all crowbars, power supplies and trigger amplifier are provided.

The high voltage power supply fault detect circuit detects over-charging of the PFN network. Other power faults (such as overcurrent) will break the power supply interlock, and result in an orderly abort sequence.

Pulse forming network and thyratron faults are detected using a fast gated comparator circuit in conjunction with a high impedance PFN voltage monitor. By detection of an abnormal PFN voltage level, shot to shot faults such as thyratron latchup are detected. This fault results in an immediate abort sequence, allowing quick shutdown of the modulator.

The output of the modulator is shunted with a varistor stack (Figure 2). This circuit element prevents tube flashover in the event of an open circuit load. A current shunt on the varistor stack and fast comparator circuitry are used to detect this fault.

The modulator is provided with a fast resistive monitor. The output of this monitor is fed into a fast gated pulse integral detection circuit (not shown in Figure 2). Detection of an abnormally high integrated voltage signal indicates an open load fault. Detection of a low pulse integrated voltage signal indicates tube flashover and shorted fault conditions.

The gated thyratron trigger generator is triggered by a low level (+20 V) pulse from the master control unit. Because of the high rate of current rise in the PFN discharge circuit a preionization pulse scheme was utilized to enhance thyratron performance. This pulse and the delayed trigger pulse are generated by solid-state circuitry incorporating over-rep and noise immunity elements. All grid bias voltages and required delays are generated internally. The thyratron reservoir was set to 6.65 V and the reservoir voltage set to 3.85 V. Although the specified levels given by EEV are 6.6 V and 4.5 volts for the thyratron under normal operating conditions, the thyratron at full charge voltage latched-up when the factory settings were used. With the heater and reservoir settings used, the thyratron recovered well within the recharge period.

3.0 Project chronology

November 1985

The preliminary design of the High Power Modulator was completed during November, and a design report was sent to NRL on 1 December 1985.

Orders were placed for many critical or long lead time items during November. Included in this category are: the thyratron, the two high voltage power supplies, the PFN capacitors, the

output pulse transformer, reset inductor, and charging inductor, the high voltage diodes, the filter capacitor, and the ceramic cylinders for the vacuum bushing.

December 1985

The package of detailed drawings for the fabrication of mechanical parts of the HPM was completed in December. These drawings covered all parts which were to be fabricated by outside vendors. Some mounting hardware for individual components was fabricated in-house as required and was not included in this drawing package. Orders for the two oil tanks (HPM and storage) were placed.

The detailed design of the thyratron heater and reservoir supplies, thyratron trigger circuits, and transformer reset system was completed. Most of the parts for these units were ordered and fabrication of these units was started.

The preliminary design of the control circuits was completed. Some of the major components for the control system were ordered.

January 1986

The balance of fabricated hardware not ordered in December was ordered in January.

Fabrication of the thyratron heater and reservoir supplies, thyratron trigger circuits, and transformer reset system was completed.

The detailed design of the control system with the exception of the fault detection circuitry was completed in January. Parts were ordered and fabrication of this unit was started.

February 1986

The assembly of the modulator itself was nearly completed during February. The installation of the input filter capacitor and the filament stepdown transformer on the modulator output were delayed due to late delivery of the components.

The construction of the thyratron cathode/reservoir power supply, thyratron trigger generator, and the power distribution chassis was completed. These chassis were the only ones which were absolutely needed before modulator testing could be initiated.

March 1986

The assembly of the modulator was completed in March with the exception of details which have nothing to do with the operation of the system.

Testing was initiated without the master controller. The self-inductance of the pulse forming network (PFN) capacitors was not determined by the manufacturer until after the final design of the high power modulator (HPM) was completed. The self-inductance was much larger than originally estimated and, therefore, required a much more aggressive taper of the PFN impedance to obtain a flat output pulse. The tuning of the PFN was complicated by an error in the installation of the PFN fault protection diodes which was identified and corrected. An eighth stage had to be added to the PFN in order to meet the pulse length specifi-

cation. This possibility was anticipated and required only minor modifications to the hardware, though it did decimate the supply of spare PFN capacitors.

Initial problems with flashover of the ceramic high voltage vacuum bushing were resolved by replacing the elastomer o-rings to eliminate leaks. A base pressure of 2×10^{-6} Torr was obtained with a 4" untrapped diffusion pump, and was probably limited by the buna-n seals used throughout the system. Occasional flashovers occurred after replacement of the seals. These flashovers had no permanent effect on the performance of the system.

Little difficultly was encountered during the initial continuous pulse train or "slow-rep" mode of operation. Pulse sequences were limited to 2000 shots because the output of the machine had to be monitored visually. The fault detection circuits were not available at this time.

The design of the fault detection circuitry was completed and fabrication was started.

April 1986

Burst mode operation was initiated in April without the master controller. The number of pulses per burst was limited to two to minimize damage in the event of a fault. It was apparent that the Peschel power supply would not be capable of providing acceptable shot-to-shot repeatability; factors of two changes in output pulse amplitude were observed from shot-to-shot. However, no problems were encountered with the modulator itself in this mode.

The master controller was installed without the fault detection circuitry (initially). This permitted easy control of operating mode, pulse repetition frequency, and pulse quantity in the burst mode.

A Peschel engineer was sent to PSI to try to bring the power supply within specifications. His attempts failed and he returned to the factory without a plan to fix the supply. PSI personnel then addressed the power supply problem and made a number of modifications to the SCR phase control and feedback circuits to improve their response time which resulted in acceptable peformance though the power supply still failed to meet the specifications written by PSI. The shot-to-shot voltage repeatability is ± 4% at 100 Hz and is approximately ± 2% at 1 Hz.

The fault detection circuitry was installed in the master controller later in April and its performance was demonstrated. This permitted extended operation of the HPM in the continuous and burst modes, since the danger of repetitive faults was removed. This capability was essential to testing of the Peschel supply.

May 1986

The modulator was intentionally operated with its output open and shorted to demonstrate that fault protection circuitry within the modulator prevents damage to modulator components under these condidtions. The ability of the fault detection circuitry of the master controller to detect these conditions and to automatically terminate a sequence of pulses even at 100 Hz repetition rates was demonstrated.

Pre-acceptance tests were performed. No difficulties were encountered in the "single shot" or "burst" modes of operation. However, two problems were encountered in extended operation at 1 Hz. Operation was interrupted by persistent tripping of the circuit breaker in the building power distribution panel. This breaker was equivalent to a 50 A, 480 V unit which was more sensitive than the 60 A breaker on the Peschel power supply. The problem was solved by replacing the building circuit breaker. After extended operation (2500 shots) one of the dummy load resistors on the output of the modulator disintegrated. The load resistors were replaced with a temporary string of resistors and the tests completed.

Acceptance tests were performed at PSI on 5 May 1986 with J. Mathew representing NRL present. The tests included operation at 250 kV in the "single shot" and "burst" modes of operation. Bursts of 50 pulses at 100 Hz were fired. The modulator was tested with its output intentionally open and shorted. Finally, the modulator was operated for 3600 pulses at 1 Hz with a 200 kV output pulse.

The modulator was disassembled and packaged following the acceptance tests. It was shipped on 16 May.

The system was unpacked and reassembled at NRL during 27-29 May.

Acceptance tests were performed at NRL on 30 May. No problems were encountered with the modulator itself. Minor problems were encountered with the control system, particularly due to thermal difficulties with the Glassman power supply and the master controller. Solutions were implimented and demonstrated on 3 June. This completed the project with the exception of reporting requirements.

4.0 TESTS

4.1 General Tests

Testing was performed into a resistive load. The thermionic diode indicated in Figure 2 was replaced by a 400-ohm fixed load. Three stackpole resistors 1" in diameter, 12" long, (oil impregnated) were mounted on the output of the transformer. In addition the vacuum bushing was left connected to evaluate the impact of the total stray capacitance on the output of the transformer. Along with the matched load tests, short circuit and open circuit tests were performed. During these tests, fault mode interrupts in the main control system were bypassed, to allow rep-rate fault mode testing. During the tests an in-situ voltage monitor was used along with a Pearson Probe (110 A) to evaluate the systems' voltage and current performance.

Figure 9 shows the superposition of 23 output voltage pulses taken at a 1 pps rep-rate. Specifically, these were shots 500-522 in a 3600 shot sequence. The PFN charge voltage was 25 kV which produces a 200 kV output pulse into a matched load. Pulse-to-pulse voltage variation is influenced by the trickle charge supply which has sufficient time to provide some regulation at rep-rates of 1 pps or less.

The voltage and current are shown in Figure 10, into a 400-ohm load. The photograph is an overlay of 50 shots during a burst mode test. The peak current was approximately 600 A peak. In addition, the peak output voltage was approximately 280 kV, ± 3% during the 1 μs pulse (PFN charge voltage 33 kV, ± 3%). Note the slight difference in the current and voltage waveshapes. Because the output of the circuit was capacitance-dominated rather than inductance limited, some slow oscillation or droop was seen on the voltage waveform. The current was flat to better

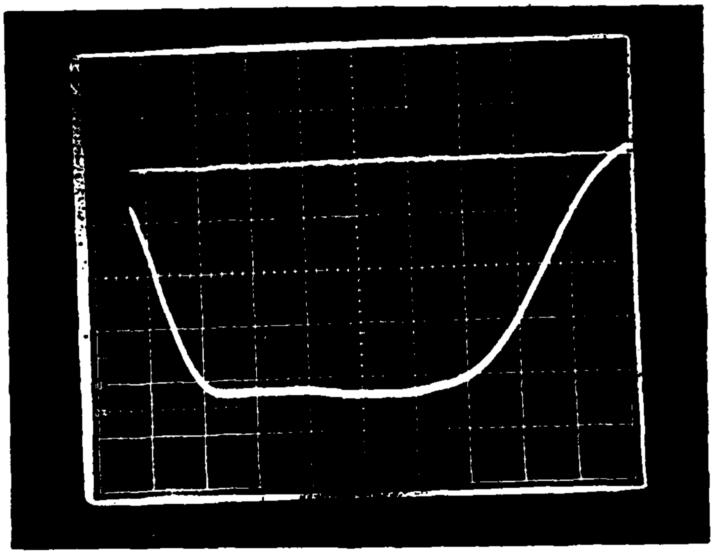

FIGURE 9. Superposition of 23 output voltage pulses taken at 1 pps. PFN charge voltage = 25 kV. Scales are 46 kV/div and 200 ns/div.

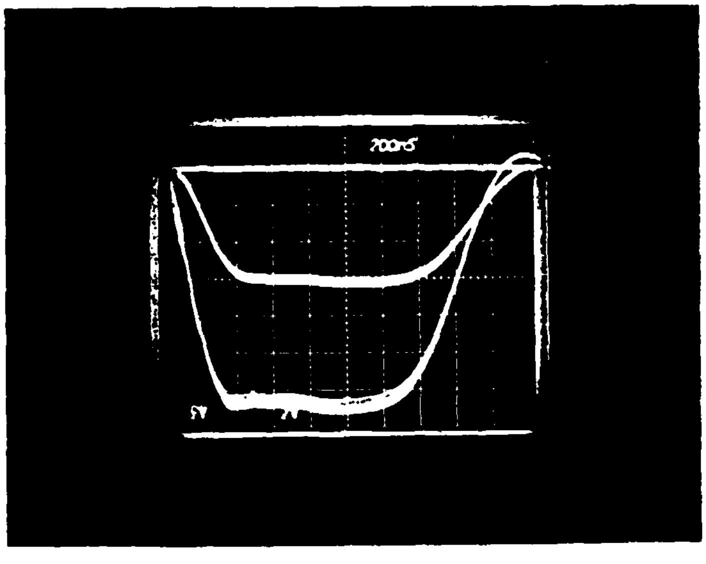

FIGURE 10. Voltage and current measurements through a 400-ohm load. The top trace is the current through the load, 200 ns/div; 200 A/div. The bottom trace is the voltage across the load, 200 ns/div, 42.5 kV/div, under 100 pps 50-pulse burst mode operation.

than ± 2%. Notice also that some amplitude variation is present on the pulses. This was a result of the power supply voltage variation and not a result of the discharge circuit.

The modulator was also tested under open circuit and short circuit fault modes. The resistive load was shorted out, and the modulator was fired several times into the short (Figure 11). The peak current was 1300 A versus the calculated current of 1275 A. The resulting thyratron current was 19.5 kA. No degradation in the modulators' performance was noted, although approximately 100 shorted shots were fired. The open circuit tests tested the validity of using high voltage MOV stacks as protection devices during open circuit shots. The secondary was open circuited by disconnecting the load. Figure 12 shows an initial transient of 460 kV present for approximately 150 ns before the MOV stack clamps the voltage to 300 kV (PFN charge voltage 35 kV). No degradation in the performance of the modulator was noted during these tests, indicating the feasibility of using passive protection schemes. In addition, because the high voltage transient only lasted for several hundred ns, no vacuum insulator breakdown was noted during the tests.

4.2 Acceptance tests at PSI

The acceptance tests preformed at PSI were defined to demonstrate compliance with the electrical specifications of the HPM. They consisted of a sequence of individual pulses fired in the "single shot" mode to demonstrate voltage variability and the electrical characteristics of a pulse, a sequence of open circuit and shorted shots to demonstrate operation of the fault mode detection circuits and the survivability of the modulator under these conditions, a sequence of bursts of 50 pulses at 100 Hz, and sustained operation at 1 Hz.

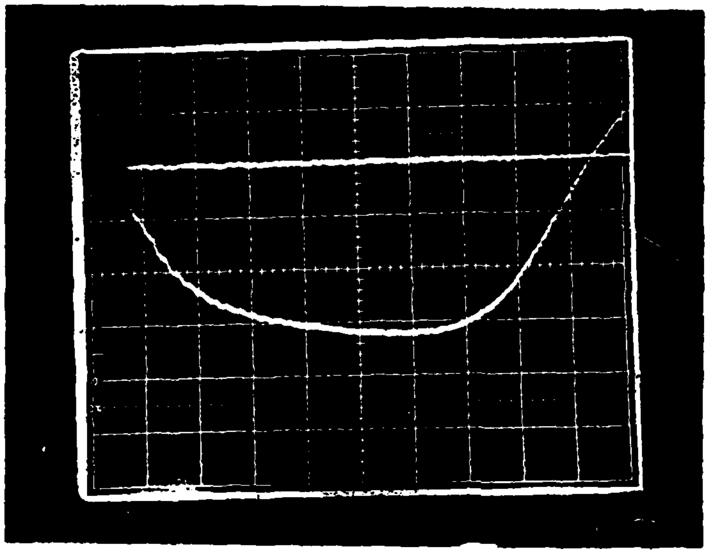

FIGURE 11. Short circuit current on the secondary of the transformer, 200 ns/div, 400 A/div (33 kV PFN charge voltage).

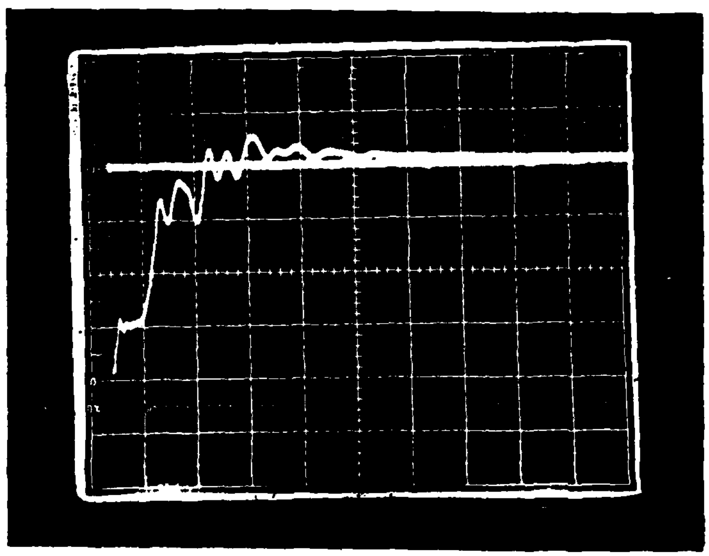

FIGURE 12. Voltage across the secondary of the transformer during an open circuit shot. During the tests the V_{PFN} = 35 kV. The initial transient is a result of the MOV turn-on time, 2 μs/div, 115 kV/div.

Three shots were fired at different PFN charge voltages to demonstrate voltage variability. The output voltage pulses generated are shown in Figures a1-a3. Several shots were fired at a PFN charge voltage of 33 kV. The resulting output voltage waveforms are shown in Figures b1-b2. The output load consisted of two resistors of 502 and 2040 ohms connected in parallel. The current measured flowing through the 502 ohm resistor is shown in Figure b4. These shots demonstrated a maximum output voltage of 270 kV, a total output current at maximum voltage of 600 A, a flattop (± 3 %) pulse duration of 1000 ns, a 10-90% risetime of 220 ns, and a 90-10% falltime of 400 ns.

Two shots were fired with the output of the modulator intentionally shorted, and two shots were fired with the modulator load disconnected. In both cases, the HPM was fired in the "burst" mode at 100 Hz to demonstrate that the fault mode detection circuitry would identify the condition and terminate the burst before a second pulse was fired. The short circuit current waveform is shown in Figure c1, and the open circuit voltage in Figure d1. The fault detection circuitry worked in all cases.

Continuous operation at 1 Hz was demonstrated at a PFN charge voltage of 25 kV which produced an output voltage of 200 kV in accordance with the minimum output voltage specification. The modulator was operated for 3600 shots (approximately one hour) in this mode. The output voltage and current were recorded at approximately 500 shot intervals. Some of the recorded data is shown in Figures e1-e19.

A total of seven 50 pulse bursts were fired at 100 Hz. The output voltage waveforms are shown in Figures f3-f9. In Figures f3-f8, the apparent timing jitter is due to the low trigger level of the oscilloscope which was set to capture the full risetime of the pulse.

A1 PFN chg 9KV

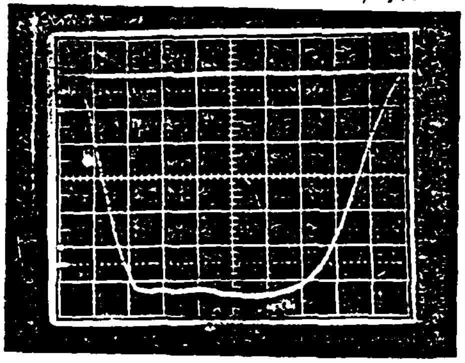

Fig. a1 - Voltage - 9kV charge - 11.5kV/,200ns/ - Single shot

B2 PFN chg 33kV

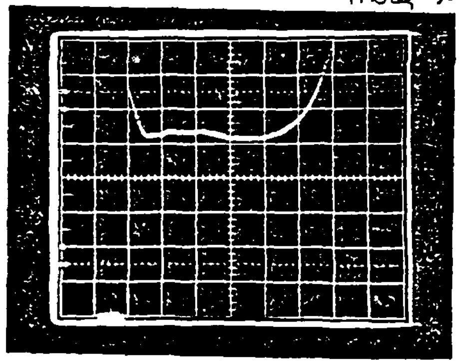

Fig. b2 - Voltage - 33kV charge - 23.0kV/,200ns/ - Single shot - Note 2

A2 PFN chg 17KV

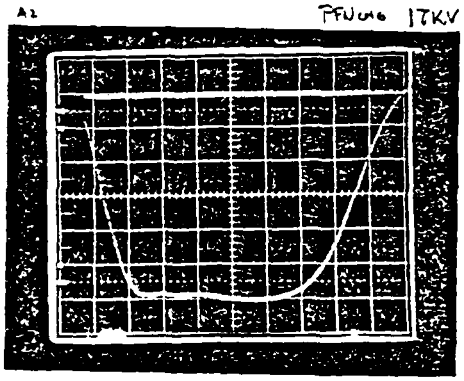

Fig. a2 - Voltage - 17kV charge - 23.0kV/,200ns/ - Single shot

B4 PFN chg 33kV

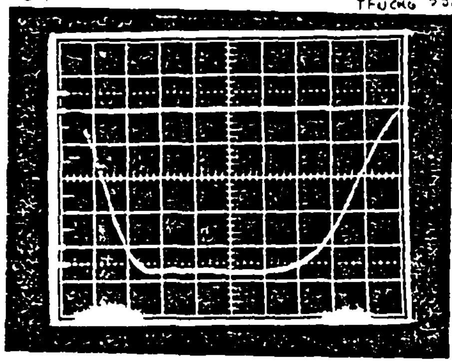

Fig. b4 - Current - 33kV charge - 100A/,200ns/ - Single shot - Note 3

A3 PFN chg 33kv

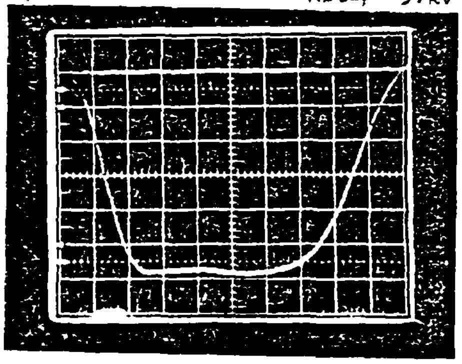

Fig. a3 - Voltage - 33kV charge - 46.0kV/,200ns/ - Single shot

C1 PFN chg 33kV

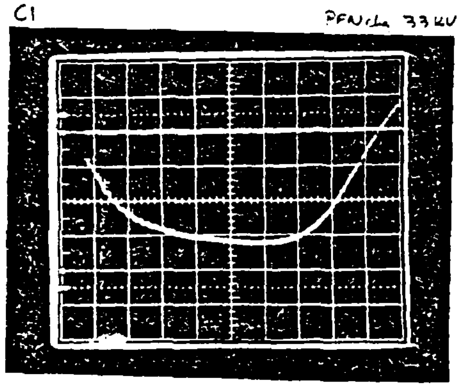

Fig. c1 - Current - 33kV charge - 400A/,200ns/ - Single shot - Short circuit

B1 PFN chg (2 shots) 33kV

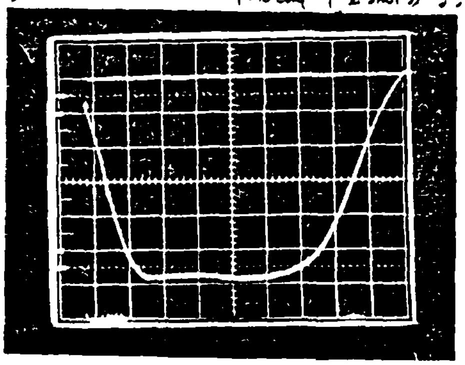

Fig. b1 - Voltage - 33kV charge - 46.0kV/,200ns/ - Single shot - Note 1

D1 PFN chg 33kV

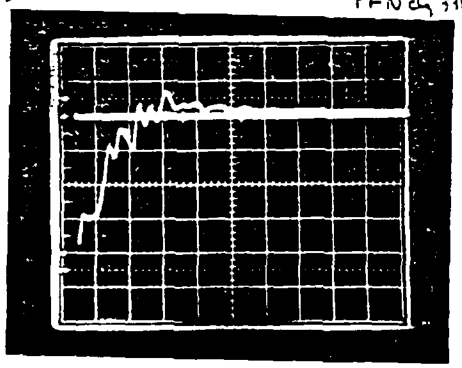

Fig. d1 - Voltage - 33kV charge - 115kV/,200ns/ - Single shot - Open circuit

E1 PFN chg 25kV

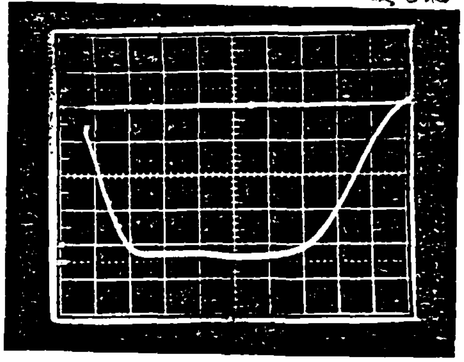

Fig. e1 - Voltage - 25kV charge - 46.0kV/,200ns/ - 1 Hz - shots 1- 10

E9 PFN CHG 25kV

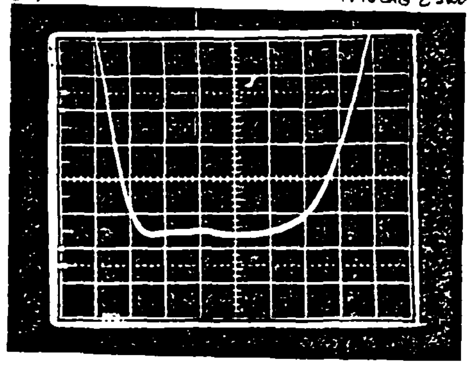

Fig. e9 - Voltage - 25kV charge - 23.0kV/,200ns. - 1 Hz - shots 2000-2014 - Note 2

E3 PFN chg 25kV

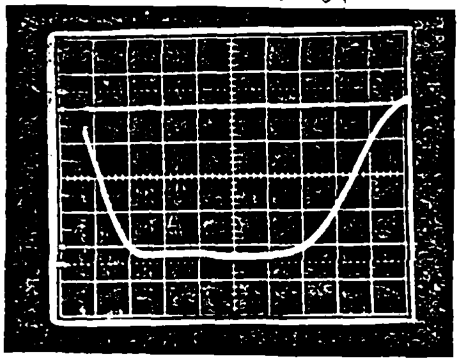

Fig. e3 - Voltage - 25kV charge - 46.0kV/,200ns/ - 1 Hz - shots 500- 522

E13 PFN CHG 25kV

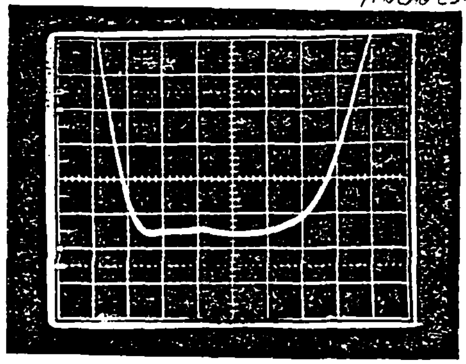

Fig. e13 - Voltage - 25kV charge - 23.0kV/,200n: - 1 Hz - shots 2600-2612 - Note 2

E4 PFN chg 25kV

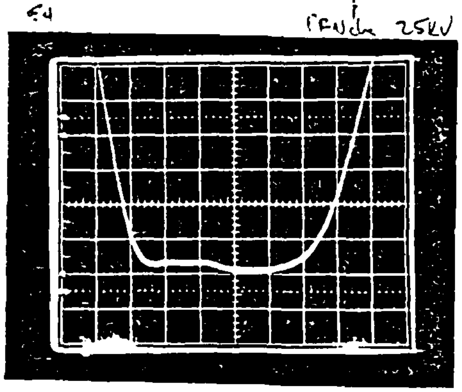

Fig. e4 - Voltage - 25kV charge - 23.0kV/,200ns/ - 1 Hz - shots 750- 762 - Note 2

E15 PFN CHG 25kV

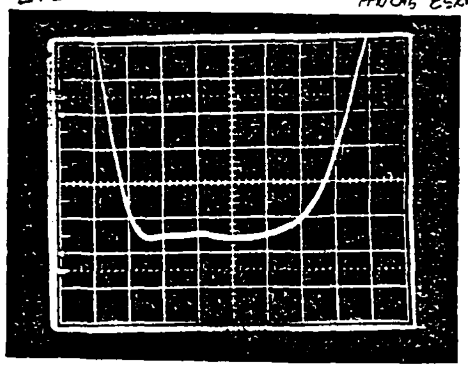

Fig. e15 - Voltage - 25kV charge - 23.0kV/,200n: - 1 Hz - shots 3000-3015 - Note 2

E7 PFN CHG 25kV

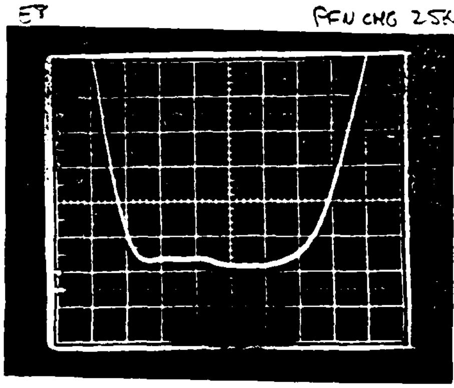

Fig. e3 - Voltage - 25kV charge - 23.0kV/,200ns/ - 1 Hz - shots 1750-1762 - Note 2

E19 PFN CHG 25kV

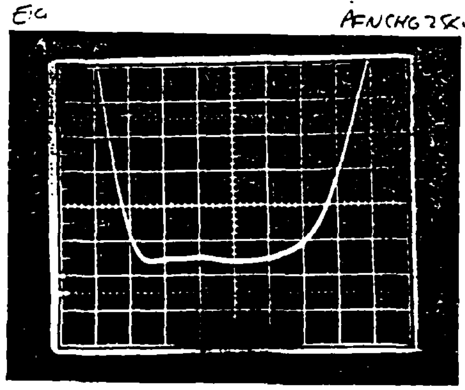

Fig. e19 - Voltage - 25kV charge - 23.0kV/,200r - 1 Hz - shots 3540-3600 - Note 2

F3 1st BURST @. PFNCHG 33KV

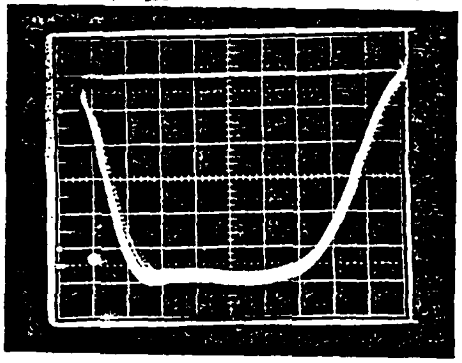

Fig. f3 - Voltage - 33kV charge - 46.0kV/,200ns/ - burst #1 - Note 4,5

F4 2ND BURST @, PFNCHG 33KV

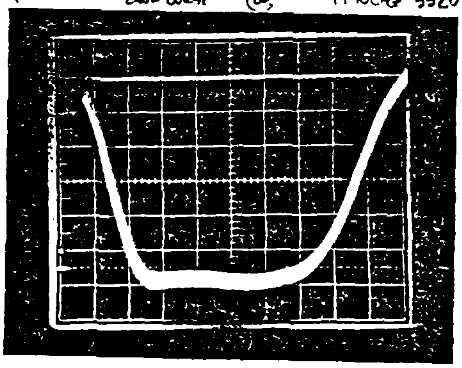

Fig. f4 - Voltage - 33kV charge - 46.0kV/,200ns/ - burst #2 - Note 4,5

F5 3RD BURST @ PFNchg 33KV

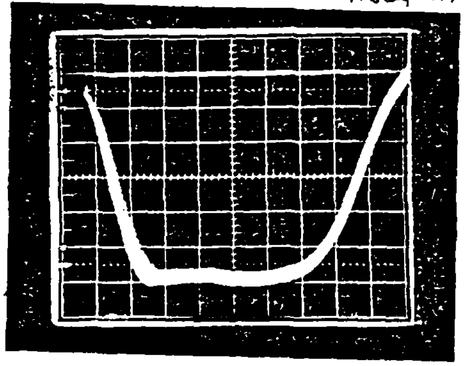

Fig. f5 - Voltage - 33kV charge - 46.0kV/,200ns/ - burst #3 - Note 4,5

4th BURST @ PFN chg 33KV

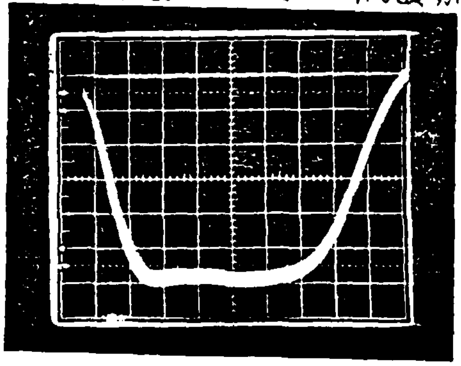

Fig. f6 - Voltage - 33kV charge - 46.0kV/,200ns/ - burst #4 - Note 4,5

F7 5th BURST @ PFNchg 33KV

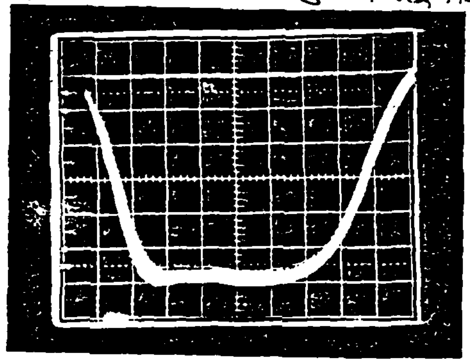

Fig. f7 - Voltage - 33kV charge - 46.0kV/,200ns/ - burst #5 - Note 4,5

F8 6th BURST @ PFNchg 33KV

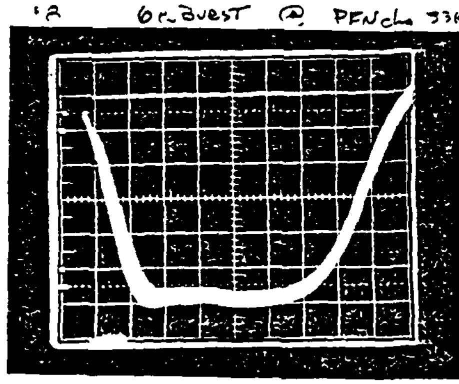

Fig. f8 - Voltage - 33kV charge - 46.0kV/,200ns/ - burst #6 - Note 4,5

BURST @PFN 33KV

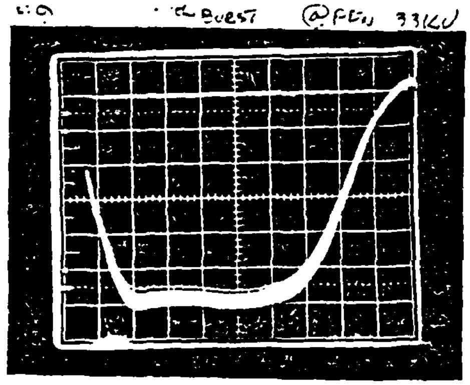

Fig. f9 - Voltage - 33kV charge - 46.0kV/,200ns/ - burst #7 - Note 4

Note - Figure numbers refer to acceptance test letter and shot number within test. Oscillograms of other shots are available but not included in this report.

Note 1 - Two shot overlay

Note 2 - The zero volt baseline was shifted off screen to permit recording the top of the pulse at a higher sensitivity.

Note 3 - The current recorded was measured through one (500 Ohm) of two parallel load resistors whose DC resistance were measured to be 503 and 2040 Ohms. Pulsed resistance is slightly higher.

Note 4 - Overlay of all pulses in a 50 pulse burst at 100 Hz

Note 5 - Apparent jitter was due to the oscilloscope trigger level which was set to record the 10% of peak amplitude portion of the pulse. See Fig. f9 for different trigger level setting.

4.3 Acceptance tests at NRL

The acceptance tests which were performed at PSI were repeated at NRL with the exception of the open circuit and short circuit tests. A number of minor problems were encountered and corrected during these tests. The most significant problem was overheating of the Glassman high voltage power supply and the HPM master controller. Ventilation in the control rack was improved and the solution of the thermal problem was verified by an additional abbreviated set of acceptance tests.

5.0 Summary

The High Power Modulator meets or exceeds all of the minimum specifications and meets or exceeds the design goals with the exception that continuous operation at 1 Hz above the minimum output voltage has not been demonstrated. A sophisticated control system provides selection of operating mode and all operating parameters as well as fault detection and automatic shut-down in the event of faults. The use of a stripline PFN and high voltage pulse transformer permits easy tuning of the output pulse to match temporal impedance profiles of electron beam loads. The ceramic high voltage vacuum bushing with metal vacuum seals is compatible with a wide range of thermionic cathodes which can be powered through multiple secondary windings of the output pulse transformer.

ACKNOWLEDGEMENTS

Phil Champney and Jim Fockler provided many valuable suggestions which were gratefully appreciated. Pulse Sciences would also like to acknowledge the help and advice provided by Hu Menown and the staff at EEV, and the excellent assistance provided by NRL during acceptance tests at their facility.

Special thanks are owed H. Lackner for invaluable assistance during the development and installation of the HPM. D. Battilana, M. Creely, D. Nett, and C. Sink did most of the assembly work. D. Pellow prepared the drawing package and assisted with the mechanical design. R. Altes performed the necessary mechanical engineering calculations and W. Weseloh performed the electrostatic modelling of the high voltage vacuum bushing. J. Clemmons was responsible for seeing that all of the parts of the HPM were available when needed.

REFERENCES

1. G. McDuff, K. Rust, "Evaluation of Bidirectionally Conducting Thyratrons for Pulsed Excimer Lasers", IEEE 16th Power Modulator Symposium, Arlington, VA, 18-20 June 1984.

2. G.W. Glasoe and J.W. Lebacqz, Pulse Generators, pg. 175-224, Dover Publications, New York, 1948.

3. Giacoletto, Electronics Designer's Handbook, pg. 3-46, McGraw-Hill, 2nd Edition, 1977.

4. Terman, Radio Engineers Handbook, McGraw-Hill, 1st Edition, New York and London, 1943.

END

10-86

DTIC